POLITECNICO DI TORINO
Repository ISTITUZIONALE

Measurements of the branching fractions of the inclusive decays D0(D+)++X

Original
Measurements of the branching fractions of the inclusive decays D0(D+)++X / Ablikim, M., Achasov, M.N., Adlarson, P., Aliberti, R., Amoroso, A., An, M.R., An, Q., Bai, Y., Bakina, O., Balossino, I., Ban, Y., Batozskaya, V., Becker, D., Begzsuren, K., Berger, N., Bertani, M., Bettoni, D., Bianchi, F., Bianco, E., Bloms, J., et al.. - In: PHYSICAL REVIEW D. - ISSN 2470-0010. - ELETTRONICO. - 107:3(2023), pp. 1-15. [10.1103/PhysRevD.107.032002]

Availability:
This version is available at: 11583/2976831 since: 2023-03-12T19:56:42Z

Publisher:
American Physical Society

Published
DOI:10.1103/PhysRevD.107.032002

Terms of use:

This article is made available under terms and conditions as specified in the corresponding bibliographic description in the repository

Publisher copyright

(Article begins on next page)

08 October 2026

Measurements of the branching fractions of the inclusive decays $D^0(D^+) \to \pi^+\pi^+\pi^- X$

M. Ablikim,[1] M. N. Achasov,[13,b] P. Adlarson,[73] R. Aliberti,[34] A. Amoroso,[72a,72c] M. R. An,[38] Q. An,[69,56] Y. Bai,[55] O. Bakina,[35] I. Balossino,[29a] Y. Ban,[45,g] V. Batozskaya,[1,43] D. Becker,[34] K. Begzsuren,[31] N. Berger,[34] M. Bertani,[28a] D. Bettoni,[29a] F. Bianchi,[72a,72c] E. Bianco,[72a,72c] J. Bloms,[66] A. Bortone,[72a,72c] I. Boyko,[35] R. A. Briere,[5] A. Brueggemann,[66] H. Cai,[74] X. Cai,[1,56] A. Calcaterra,[28a] G. F. Cao,[1,61] N. Cao,[1,61] S. A. Cetin,[60a] J. F. Chang,[1,56] W. L. Chang,[1,61] G. R. Che,[42] G. Chelkov,[35,a] C. Chen,[42] Chao Chen,[53] G. Chen,[1] H. S. Chen,[1,61] M. L. Chen,[1,56,61] S. J. Chen,[41] S. M. Chen,[59] T. Chen,[1,61] X. R. Chen,[30,61] X. T. Chen,[1,61] Y. B. Chen,[1,56] Y. Q. Chen,[33] Z. J. Chen,[25,h] W. S. Cheng,[72c] S. K. Choi,[53] X. Chu,[42] G. Cibinetto,[29a] S. C. Coen,[4] F. Cossio,[72c] J. J. Cui,[48] H. L. Dai,[1,56] J. P. Dai,[77] A. Dbeyssi,[19] R. E. de Boer,[4] D. Dedovich,[35] Z. Y. Deng,[1] A. Denig,[34] I. Denysenko,[35] M. Destefanis,[72a,72c] F. De Mori,[72a,72c] B. Ding,[64,1] Y. Ding,[39] Y. Ding,[33] J. Dong,[1,56] L. Y. Dong,[1,61] M. Y. Dong,[1,56,61] X. Dong,[74] S. X. Du,[79] Z. H. Duan,[41] P. Egorov,[35,a] Y. L. Fan,[74] J. Fang,[1,56] S. S. Fang,[1,61] W. X. Fang,[1] Y. Fang,[1] R. Farinelli,[29a] L. Fava,[72b,72c] F. Feldbauer,[4] G. Felici,[28a] C. Q. Feng,[69,56] J. H. Feng,[57] K. Fischer,[67] M. Fritsch,[4] C. Fritzsch,[66] C. D. Fu,[1] Y. W. Fu,[1] H. Gao,[61] Y. N. Gao,[45,g] Yang Gao,[69,56] S. Garbolino,[72c] I. Garzia,[29a,29b] P. T. Ge,[74] Z. W. Ge,[41] C. Geng,[57] E. M. Gersabeck,[65] A. Gilman,[67] K. Goetzen,[14] L. Gong,[39] W. X. Gong,[1,56] W. Gradl,[34] M. Greco,[72a,72c] M. H. Gu,[1,56] Y. T. Gu,[16] C. Y. Guan,[1,61] Z. L. Guan,[22] A. Q. Guo,[30,61] L. B. Guo,[40] R. P. Guo,[47] Y. P. Guo,[12,f] A. Guskov,[35,a] X. T. H.,[1,61] W. Y. Han,[38] X. Q. Hao,[20] F. A. Harris,[63] K. K. He,[53] K. L. He,[1,61] F. H. Heinsius,[4] C. H. Heinz,[34] Y. K. Heng,[1,56,61] C. Herold,[58] T. Holtmann,[4] P. C. Hong,[12,f] G. Y. Hou,[1,61] Y. R. Hou,[61] Z. L. Hou,[1] H. M. Hu,[1,61] J. F. Hu,[54,i] T. Hu,[1,56,61] Y. Hu,[1] G. S. Huang,[69,56] K. X. Huang,[57] L. Q. Huang,[30,61] X. T. Huang,[48] Y. P. Huang,[1] T. Hussain,[71] N. Hüsken,[27,34] W. Imoehl,[27] M. Irshad,[69,56] J. Jackson,[27] S. Jaeger,[4] S. Janchiv,[31] E. Jang,[53] J. H. Jeong,[53] J. H. Jeong,[10] Q. Ji,[1] Q. P. Ji,[20] X. B. Ji,[1,61] X. L. Ji,[1,56] Y. Y. Ji,[48] Z. K. Jia,[69,56] P. C. Jiang,[45,g] S. S. Jiang,[38] T. J. Jiang,[17] X. S. Jiang,[1,56,61] Y. Jiang,[61] J. B. Jiao,[48] Z. Jiao,[23] S. Jin,[41] Y. Jin,[64] M. Q. Jing,[1,61] T. Johansson,[73] X. K.,[1] S. Kabana,[32] N. Kalantar-Nayestanaki,[62] X. L. Kang,[9] X. S. Kang,[39] R. Kappert,[62] M. Kavatsyuk,[62] B. C. Ke,[79] A. Khoukaz,[66] R. Kiuchi,[1] R. Kliemt,[14] L. Koch,[36] O. B. Kolcu,[60a] B. Kopf,[4] M. Kuessner,[4] A. Kupsc,[43,73] W. Kühn,[36] J. J. Lane,[65] J. S. Lange,[36] P. Larin,[19] A. Lavania,[26] L. Lavezzi,[72a,72c] T. T. Lei,[69,k] Z. H. Lei,[69,56] H. Leithoff,[34] M. Lellmann,[34] T. Lenz,[34] C. Li,[42] C. Li,[46] C. H. Li,[38] Cheng Li,[69,56] D. M. Li,[79] F. Li,[1,56] G. Li,[1] H. Li,[69,56] H. B. Li,[1,61] H. J. Li,[20] H. N. Li,[54,i] Hui Li,[42] J. R. Li,[59] J. S. Li,[57] J. W. Li,[48] Ke Li,[1] L. J. Li,[1,61] L. K. Li,[1] Lei Li,[3] M. H. Li,[42] P. R. Li,[37,j,k] S. X. Li,[12] S. Y. Li,[59] T. Li,[48] W. D. Li,[1,61] W. G. Li,[1] X. H. Li,[69,56] X. L. Li,[48] Xiaoyu Li,[1,61] Y. G. Li,[45,g] Z. J. Li,[57] Z. X. Li,[16] Z. Y. Li,[57] C. Liang,[41] H. Liang,[33] H. Liang,[1,61] H. Liang,[69,56] Y. F. Liang,[52] Y. T. Liang,[30,61] G. R. Liao,[15] L. Z. Liao,[48] J. Libby,[26] A. Limphirat,[58] D. X. Lin,[30,61] T. Lin,[1] B. X. Liu,[74] B. J. Liu,[1] C. Liu,[33] C. X. Liu,[1] D. Liu,[19,69] F. H. Liu,[51] Fang Liu,[1] Feng Liu,[6] G. M. Liu,[54,i] H. Liu,[37,j,k] H. B. Liu,[16] H. M. Liu,[1,61] Huanhuan Liu,[1] Huihui Liu,[21] J. B. Liu,[69,56] J. L. Liu,[70] J. Y. Liu,[1,61] K. Liu,[1] K. Y. Liu,[39] Ke Liu,[22] L. Liu,[69,56] L. C. Liu,[42] Lu Liu,[42] M. H. Liu,[12,f] P. L. Liu,[1] Q. Liu,[61] S. B. Liu,[69,56] T. Liu,[12,f] W. K. Liu,[42] W. M. Liu,[69,56] X. Liu,[37,j,k] Y. Liu,[37,j,k] Y. B. Liu,[42] Z. A. Liu,[1,56,61] Z. Q. Liu,[48] X. C. Lou,[1,56,61] F. X. Lu,[57] H. J. Lu,[23] J. G. Lu,[1,56] X. L. Lu,[1] Y. Lu,[7] Y. P. Lu,[1,56] Z. H. Lu,[1,61] C. L. Luo,[40] M. X. Luo,[78] T. Luo,[12,f] X. L. Luo,[1,56] X. R. Lyu,[61] Y. F. Lyu,[42] F. C. Ma,[39] H. L. Ma,[1] J. L. Ma,[1,61] L. L. Ma,[48] M. M. Ma,[1,61] Q. M. Ma,[1] R. Q. Ma,[1,61] R. T. Ma,[61] X. Y. Ma,[1,56] Y. Ma,[45,g] F. E. Maas,[19] M. Maggiora,[72a,72c] S. Maldaner,[4] S. Malde,[67] A. Mangoni,[28b] Y. J. Mao,[45,g] Z. P. Mao,[1] S. Marcello,[72a,72c] Z. X. Meng,[64] J. G. Messchendorp,[14,62] G. Mezzadri,[29a] H. Miao,[1,61] T. J. Min,[41] R. E. Mitchell,[27] X. H. Mo,[1,56,61] N. Yu. Muchnoi,[13,b] Y. Nefedov,[35] F. Nerling,[19,d] I. B. Nikolaev,[13,b] Z. Ning,[1,56] S. Nisar,[11,l] Y. Niu,[48] S. L. Olsen,[61] Q. Ouyang,[1,56,61] S. Pacetti,[28b,28c] X. Pan,[53] Y. Pan,[55] A. Pathak,[33] Y. P. Pei,[69,56] M. Pelizaeus,[4] H. P. Peng,[69,56] K. Peters,[14,d] J. L. Ping,[40] R. G. Ping,[1,61] S. Plura,[34] S. Pogodin,[35] V. Prasad,[69,56] V. Prasad,[32] F. Z. Qi,[1] H. Qi,[69,56] H. R. Qi,[59] M. Qi,[41] T. Y. Qi,[12,f] S. Qian,[1,56] W. B. Qian,[61] C. F. Qiao,[61] J. J. Qin,[70] L. Q. Qin,[15] X. P. Qin,[12,f] X. S. Qin,[48] Z. H. Qin,[1,56] J. F. Qiu,[1] S. Q. Qu,[59] C. F. Redmer,[34] K. J. Ren,[38] A. Rivetti,[72c] V. Rodin,[62] M. Rolo,[72c] G. Rong,[1,61] Ch. Rosner,[19] S. N. Ruan,[42] A. Sarantsev,[35,c] Y. Schelhaas,[34] K. Schoenning,[73] M. Scodeggio,[29a,29b] K. Y. Shan,[12,f] W. Shan,[24] X. Y. Shan,[69,56] J. F. Shangguan,[53] L. G. Shao,[1,61] M. Shao,[69,56] C. P. Shen,[12,f] H. F. Shen,[1,61] W. H. Shen,[61] X. Y. Shen,[1,61] B. A. Shi,[61] H. C. Shi,[69,56] J. Y. Shi,[1] Q. Q. Shi,[53] R. S. Shi,[1,61] X. Shi,[1,56] J. J. Song,[20] T. Z. Song,[57] W. M. Song,[33,1] Y. X. Song,[45,g] S. Sosio,[72a,72c] S. Spataro,[72a,72c] F. Stieler,[34] Y. J. Su,[61] G. B. Sun,[74] G. X. Sun,[1] H. Sun,[61] H. K. Sun,[1] J. F. Sun,[20] K. Sun,[59] L. Sun,[74] S. S. Sun,[1,61] T. Sun,[1,61] W. Y. Sun,[33] Y. Sun,[9] Y. J. Sun,[69,56] Y. Z. Sun,[1] Z. T. Sun,[48] Y. X. Tan,[69,56] C. J. Tang,[52] G. Y. Tang,[1] J. Tang,[57] Y. A. Tang,[74] L. Y. Tao,[70] Q. T. Tao,[25,h] M. Tat,[67] J. X. Teng,[69,56] V. Thoren,[73] W. H. Tian,[57] W. H. Tian,[50] Y. Tian,[30,61] Z. F. Tian,[74] I. Uman,[60b] B. Wang,[69,56] B. Wang,[1] B. L. Wang,[61] C. W. Wang,[41] D. Y. Wang,[45,g] F. Wang,[70] H. J. Wang,[37,j,k] H. P. Wang,[1,61] K. Wang,[1,56] L. L. Wang,[1] M. Wang,[48] Meng Wang,[1,61] S. Wang,[12,f] T. Wang,[12,f] T. J. Wang,[42] W. Wang,[57] W. Wang,[70] W. H. Wang,[74] W. P. Wang,[69,56]

X. Wang,[45,g] X. F. Wang,[37,j,k] X. J. Wang,[38] X. L. Wang,[12,f] Y. Wang,[59] Y. D. Wang,[44] Y. F. Wang,[1,56,61] Y. H. Wang,[46] Y. N. Wang,[44] Y. Q. Wang,[1] Yaqian Wang,[18,1] Yi Wang,[59] Z. Wang,[1,56] Z. L. Wang,[70] Z. Y. Wang,[1,61] Ziyi Wang,[61] D. Wei,[68] D. H. Wei,[15] F. Weidner,[66] S. P. Wen,[1] C. W. Wenzel,[4] D. J. White,[65] U. Wiedner,[4] G. Wilkinson,[67] M. Wolke,[73] L. Wollenberg,[4] C. Wu,[38] J. F. Wu,[1,61] L. H. Wu,[1] L. J. Wu,[1,61] X. Wu,[12,f] X. H. Wu,[33] Y. Wu,[69] Y. J. Wu,[30] Z. Wu,[1,56] L. Xia,[69,56] X. M. Xian,[38] T. Xiang,[45,g] D. Xiao,[37,j,k] G. Y. Xiao,[41] H. Xiao,[12,f] S. Y. Xiao,[1] Y. L. Xiao,[12,f] Z. J. Xiao,[40] C. Xie,[41] X. H. Xie,[45,g] Y. Xie,[48] Y. G. Xie,[1,56] Y. H. Xie,[6] Z. P. Xie,[69,56] T. Y. Xing,[1,61] C. F. Xu,[1,61] C. J. Xu,[57] G. F. Xu,[1] H. Y. Xu,[64] Q. J. Xu,[17] W. L. Xu,[64] X. P. Xu,[53] Y. C. Xu,[76] Z. P. Xu,[41] F. Yan,[12,f] L. Yan,[12,f] W. B. Yan,[69,56] W. C. Yan,[79] X. Q. Yan,[1] H. J. Yang,[49,e] H. L. Yang,[33] H. X. Yang,[1] Tao Yang,[1] Y. Yang,[12,f] Y. F. Yang,[42] Y. X. Yang,[1,61] Yifan Yang,[1,61] M. Ye,[1,56] M. H. Ye,[8] J. H. Yin,[1] Z. Y. You,[57] B. X. Yu,[1,56,61] C. X. Yu,[42] G. Yu,[1,61] T. Yu,[70] X. D. Yu,[45,g] C. Z. Yuan,[1,61] L. Yuan,[2] S. C. Yuan,[1] X. Q. Yuan,[1] Y. Yuan,[1,61] Z. Y. Yuan,[57] C. X. Yue,[38] A. A. Zafar,[71] F. R. Zeng,[48] X. Zeng,[12,f] Y. Zeng,[25,h] X. Y. Zhai,[33] Y. H. Zhan,[57] A. Q. Zhang,[1,61] B. L. Zhang,[1,61] B. X. Zhang,[1] D. H. Zhang,[42] G. Y. Zhang,[20] H. Zhang,[69] H. H. Zhang,[33] H. H. Zhang,[57] H. Q. Zhang,[1,56,61] H. Y. Zhang,[1,56] J. J. Zhang,[50] J. L. Zhang,[75] J. Q. Zhang,[40] J. W. Zhang,[1,56,61] J. X. Zhang,[37,j,k] J. Y. Zhang,[1] J. Z. Zhang,[1,61] Jiawei Zhang,[1,61] L. M. Zhang,[59] L. Q. Zhang,[57] Lei Zhang,[41] P. Zhang,[1] Q. Y. Zhang,[38,79] Shuihan Zhang,[1,61] Shulei Zhang,[25,h] X. D. Zhang,[44] X. M. Zhang,[1] X. Y. Zhang,[48] X. Y. Zhang,[53] Y. Zhang,[67] Y. T. Zhang,[79] Y. H. Zhang,[1,56] Yan Zhang,[69,56] Yao Zhang,[1] Z. H. Zhang,[1] Z. L. Zhang,[33] Z. Y. Zhang,[42] Z. Y. Zhang,[74] G. Zhao,[1] J. Zhao,[38] J. Y. Zhao,[1,61] J. Z. Zhao,[1,56] Lei Zhao,[69,56] Ling Zhao,[1] M. G. Zhao,[42] S. J. Zhao,[79] Y. B. Zhao,[1,56] Y. X. Zhao,[30,61] Z. G. Zhao,[69,56] A. Zhemchugov,[35,a] B. Zheng,[70] J. P. Zheng,[1,56] W. J. Zheng,[1,61] Y. H. Zheng,[61] B. Zhong,[40] X. Zhong,[57] H. Zhou,[48] L. P. Zhou,[1,61] X. Zhou,[74] X. K. Zhou,[61] X. R. Zhou,[69,56] X. Y. Zhou,[38] Y. Z. Zhou,[12,f] J. Zhu,[42] K. Zhu,[1] K. J. Zhu,[1,56,61] L. Zhu,[33] L. X. Zhu,[61] S. H. Zhu,[68] S. Q. Zhu,[41] T. J. Zhu,[12,f] W. J. Zhu,[12,f] Y. C. Zhu,[69,56] Z. A. Zhu,[1,61] J. H. Zou,[1] and J. Zu[69,56]

(BESIII Collaboration)

[1]*Institute of High Energy Physics, Beijing 100049, People's Republic of China*
[2]*Beihang University, Beijing 100191, People's Republic of China*
[3]*Beijing Institute of Petrochemical Technology, Beijing 102617, People's Republic of China*
[4]*Bochum Ruhr-University, D-44780 Bochum, Germany*
[5]*Carnegie Mellon University, Pittsburgh, Pennsylvania 15213, USA*
[6]*Central China Normal University, Wuhan 430079, People's Republic of China*
[7]*Central South University, Changsha 410083, People's Republic of China*
[8]*China Center of Advanced Science and Technology, Beijing 100190, People's Republic of China*
[9]*China University of Geosciences, Wuhan 430074, People's Republic of China*
[10]*Chung-Ang University, Seoul, 06974, Republic of Korea*
[11]*COMSATS University Islamabad, Lahore Campus, Defence Road, Off Raiwind Road, 54000 Lahore, Pakistan*
[12]*Fudan University, Shanghai 200433, People's Republic of China*
[13]*G.I. Budker Institute of Nuclear Physics SB RAS (BINP), Novosibirsk 630090, Russia*
[14]*GSI Helmholtzcentre for Heavy Ion Research GmbH, D-64291 Darmstadt, Germany*
[15]*Guangxi Normal University, Guilin 541004, People's Republic of China*
[16]*Guangxi University, Nanning 530004, People's Republic of China*
[17]*Hangzhou Normal University, Hangzhou 310036, People's Republic of China*
[18]*Hebei University, Baoding 071002, People's Republic of China*
[19]*Helmholtz Institute Mainz, Staudingerweg 18, D-55099 Mainz, Germany*
[20]*Henan Normal University, Xinxiang 453007, People's Republic of China*
[21]*Henan University of Science and Technology, Luoyang 471003, People's Republic of China*
[22]*Henan University of Technology, Zhengzhou 450001, People's Republic of China*
[23]*Huangshan College, Huangshan 245000, People's Republic of China*
[24]*Hunan Normal University, Changsha 410081, People's Republic of China*
[25]*Hunan University, Changsha 410082, People's Republic of China*
[26]*Indian Institute of Technology Madras, Chennai 600036, India*
[27]*Indiana University, Bloomington, Indiana 47405, USA*
[28a]*INFN Laboratori Nazionali di Frascati, I-00044 Frascati, Italy*
[28b]*INFN Sezione di Perugia, I-06100 Perugia, Italy*
[28c]*University of Perugia, I-06100 Perugia, Italy*

[29a]INFN Sezione di Ferrara, I-44122 Ferrara, Italy
[29b]University of Ferrara, I-44122 Ferrara, Italy
[30]Institute of Modern Physics, Lanzhou 730000, People's Republic of China
[31]Institute of Physics and Technology, Peace Avenue 54B, Ulaanbaatar 13330, Mongolia
[32]Instituto de Alta Investigación, Universidad de Tarapacá, Casilla 7D, Arica 1000000, Chile
[33]Jilin University, Changchun 130012, People's Republic of China
[34]Johannes Gutenberg University of Mainz, Johann-Joachim-Becher-Weg 45, D-55099 Mainz, Germany
[35]Joint Institute for Nuclear Research, 141980 Dubna, Moscow region, Russia
[36]Justus-Liebig-Universitaet Giessen, II. Physikalisches Institut, Heinrich-Buff-Ring 16, D-35392 Giessen, Germany
[37]Lanzhou University, Lanzhou 730000, People's Republic of China
[38]Liaoning Normal University, Dalian 116029, People's Republic of China
[39]Liaoning University, Shenyang 110036, People's Republic of China
[40]Nanjing Normal University, Nanjing 210023, People's Republic of China
[41]Nanjing University, Nanjing 210093, People's Republic of China
[42]Nankai University, Tianjin 300071, People's Republic of China
[43]National Centre for Nuclear Research, Warsaw 02-093, Poland
[44]North China Electric Power University, Beijing 102206, People's Republic of China
[45]Peking University, Beijing 100871, People's Republic of China
[46]Qufu Normal University, Qufu 273165, People's Republic of China
[47]Shandong Normal University, Jinan 250014, People's Republic of China
[48]Shandong University, Jinan 250100, People's Republic of China
[49]Shanghai Jiao Tong University, Shanghai 200240, People's Republic of China
[50]Shanxi Normal University, Linfen 041004, People's Republic of China
[51]Shanxi University, Taiyuan 030006, People's Republic of China
[52]Sichuan University, Chengdu 610064, People's Republic of China
[53]Soochow University, Suzhou 215006, People's Republic of China
[54]South China Normal University, Guangzhou 510006, People's Republic of China
[55]Southeast University, Nanjing 211100, People's Republic of China
[56]State Key Laboratory of Particle Detection and Electronics, Beijing 100049, Hefei 230026, People's Republic of China
[57]Sun Yat-Sen University, Guangzhou 510275, People's Republic of China
[58]Suranaree University of Technology, University Avenue 111, Nakhon Ratchasima 30000, Thailand
[59]Tsinghua University, Beijing 100084, People's Republic of China
[60a]Turkish Accelerator Center Particle Factory Group, Istinye University, 34010, Istanbul, Turkey
[60b]Near East University, Nicosia, North Cyprus, 99138, Mersin 10, Turkey
[61]University of Chinese Academy of Sciences, Beijing 100049, People's Republic of China
[62]University of Groningen, NL-9747 AA Groningen, The Netherlands
[63]University of Hawaii, Honolulu, Hawaii 96822, USA
[64]University of Jinan, Jinan 250022, People's Republic of China
[65]University of Manchester, Oxford Road, Manchester, M13 9PL, United Kingdom
[66]University of Muenster, Wilhelm-Klemm-Strasse 9, 48149 Muenster, Germany
[67]University of Oxford, Keble Road, Oxford OX13RH, United Kingdom
[68]University of Science and Technology Liaoning, Anshan 114051, People's Republic of China
[69]University of Science and Technology of China, Hefei 230026, People's Republic of China
[70]University of South China, Hengyang 421001, People's Republic of China
[71]University of the Punjab, Lahore-54590, Pakistan
[72a]University of Turin, I-10125 Turin, Italy
[72b]University of Eastern Piedmont, I-15121 Alessandria, Italy
[72c]INFN, I-10125 Turin, Italy
[73]Uppsala University, Box 516, SE-75120 Uppsala, Sweden
[74]Wuhan University, Wuhan 430072, People's Republic of China
[75]Xinyang Normal University, Xinyang 464000, People's Republic of China
[76]Yantai University, Yantai 264005, People's Republic of China
[77]Yunnan University, Kunming 650500, People's Republic of China

[78]*Zhejiang University, Hangzhou 310027, People's Republic of China*
[79]*Zhengzhou University, Zhengzhou 450001, People's Republic of China*

(Received 9 January 2023; accepted 19 January 2023; published 13 February 2023)

Using e^+e^- annihilation data corresponding to an integrated luminosity of 2.93 fb^{-1} taken at a center-of-mass energy of 3.773 GeV with the BESIII detector, we report the first measurements of the branching fractions of the inclusive decays $D^0 \to \pi^+\pi^+\pi^-X$ and $D^+ \to \pi^+\pi^+\pi^-X$, where pions from K^0_S decays have been excluded from the $\pi^+\pi^+\pi^-$ system and X denotes any possible particle combination. The branching fractions of $D^0(D^+) \to \pi^+\pi^+\pi^-X$ are determined to be $\mathcal{B}(D^0 \to \pi^+\pi^+\pi^-X) = (17.60 \pm 0.11 \pm 0.22)\%$ and $\mathcal{B}(D^+ \to \pi^+\pi^+\pi^-X) = (15.25 \pm 0.09 \pm 0.18)\%$, where the first uncertainties are statistical and the second systematic.

DOI: 10.1103/PhysRevD.107.032002

I. INTRODUCTION

In recent years, tests of lepton flavor universality (LFU) have become a very hot topic in heavy flavor physics. The world averages of the ratios $R(D) = \mathcal{B}(B \to D\tau\nu_\tau)/\mathcal{B}(B \to D\ell\nu_\ell)$ and $R(D^*) = \mathcal{B}(B \to D^*\tau\nu_\tau)/\mathcal{B}(B \to D^*\ell\nu_\ell)$, with $\ell = e$ or μ, deviate from the Standard Model (SM) predictions by more than 1.4σ and 2.8σ, respectively [1]. Additionally, the LHCb experiment reported the ratio of branching fractions, $R(D^{*-}) = \mathcal{B}(B^0 \to D^{*-}\tau^+\nu_\tau)/\mathcal{B}(B^0 \to D^{*-}\mu^+\nu_\mu)$, based on 3 fb^{-1} of pp data taken at 7 and 8 TeV (run I) [2,3], which had the smallest statistical uncertainty at the time and was consistent with the SM prediction within 1.1σ. However, the LHCb measurement is limited by the knowledge of the normalization channel $\mathcal{B}(B^0 \to D^{*-}\pi^+\pi^+\pi^-)$. Future data taken at the Belle II and LHCb experiments will help to further improve the accuracy of the branching fractions and tests of LFU.

In these tests, the analyses adopt the decay chain of $B^0 \to D^{*-}\tau^+\nu_\tau$ with $\tau^+ \to \pi^+\pi^+\pi^-\bar{\nu}_\tau$, where the leading and subleading background sources are from $B^{0,+} \to D_s^+ + \textit{anything}$ with $D_s^+ \to \pi^+\pi^+\pi^-X$ and $B^{0,+} \to D^0(D^+) + \textit{anything}$ with $D^0(D^+) \to \pi^+\pi^+\pi^-X$ (where $\pi^\pm$s from K^0_S decays have been excluded from $\pi^+\pi^+\pi^-$ and X denotes any possible particle combination), respectively. Unfortunately, information on inclusive decays of charmed mesons into final states containing $\pi^+\pi^+\pi^-$ is sparse. Measurements of the full and partial decay branching fractions of the inclusive decays $D_s^+ \to \pi^+\pi^+\pi^-X$ and $D^0(D^+) \to \pi^+\pi^+\pi^-X$ offer important inputs to precisely test LFU with semileptonic B decays.

Recently, the BESIII collaboration reported the first measurement of the branching fraction of the inclusive decay $D_s^+ \to \pi^+\pi^+\pi^-X$ [4]. The branching fraction obtained is greater than the sum of the branching fractions of the known exclusive D_s^+ decays containing $\pi^+\pi^+\pi^-$ by around 25%, thereby implying that many exclusive D_s^+ decays containing $\pi^+\pi^+\pi^-$ are still unmeasured. The sums of the branching fractions of the known exclusive D^0 and D^+ decays containing $\pi^+\pi^+\pi^-$ [5–8], as summarized in the Appendix, are $(16.05 \pm 0.47)\%$ and $(14.74 \pm 0.53)\%$, respectively. The measurements of the branching fractions of the inclusive decays $D^0(D^+)$ can offer a check on the known exclusive $D^0(D^+)$ decays containing $\pi^+\pi^+\pi^-$. A measurable difference between the branching fractions of inclusive and exclusive decays would indicate that either some exclusive decays are not measured or that some known exclusive decays are overestimated.

In this paper, we report the first measurements of the branching fractions of $D^0 \to \pi^+\pi^+\pi^-X$ and $D^+ \to \pi^+\pi^+\pi^-X$ by analyzing 2.93 fb^{-1} of e^+e^- collision

[a]Also at the Moscow Institute of Physics and Technology, Moscow 141700, Russia.
[b]Also at the Novosibirsk State University, Novosibirsk, 630090, Russia.
[c]Also at the NRC "Kurchatov Institute," PNPI, 188300, Gatchina, Russia.
[d]Also at Goethe University Frankfurt, 60323 Frankfurt am Main, Germany.
[e]Also at Key Laboratory for Particle Physics, Astrophysics and Cosmology, Ministry of Education; Shanghai Key Laboratory for Particle Physics and Cosmology; Institute of Nuclear and Particle Physics, Shanghai 200240, People's Republic of China.
[f]Also at Key Laboratory of Nuclear Physics and Ion-beam Application (MOE) and Institute of Modern Physics, Fudan University, Shanghai 200443, People's Republic of China.
[g]Also at State Key Laboratory of Nuclear Physics and Technology, Peking University, Beijing 100871, People's Republic of China.
[h]Also at School of Physics and Electronics, Hunan University, Changsha 410082, China.
[i]Also at Guangdong Provincial Key Laboratory of Nuclear Science, Institute of Quantum Matter, South China Normal University, Guangzhou 510006, China.
[j]Also at Frontiers Science Center for Rare Isotopes, Lanzhou University, Lanzhou 730000, People's Republic of China.
[k]Also at Lanzhou Center for Theoretical Physics, Lanzhou University, Lanzhou 730000, People's Republic of China.
[l]Also at the Department of Mathematical Sciences, IBA, Karachi, Pakistan.

Published by the American Physical Society under the terms of the Creative Commons Attribution 4.0 International license. Further distribution of this work must maintain attribution to the author(s) and the published article's title, journal citation, and DOI. Funded by SCOAP³.

data [9] taken at a center-of-mass energy of 3.773 GeV with the BESIII detector. Throughout this paper, charge conjugate decays are always implied.

II. BESIII DETECTOR AND MONTE CARLO SIMULATION

The BESIII detector is a magnetic spectrometer [10] located at the Beijing Electron Positron Collider (BEPCII) [11]. The cylindrical core of the BESIII detector consists of a helium-based multilayer drift chamber (MDC), a plastic scintillator time-of-flight system (TOF), and a CsI (Tl) electromagnetic calorimeter (EMC), which are all enclosed in a superconducting solenoidal magnet providing a 1.0 T magnetic field [12]. The solenoid is supported by an octagonal flux-return yoke with resistive plate counter muon identifier modules interleaved with steel. The solid angle coverage for detecting charged particles is 93% over 4π. The charged-particle momentum resolution at 1 GeV/c is 0.5%, and the resolution of the specific ionization energy loss (dE/dx) is 6% for the electrons from Bhabha scattering. The EMC measures photon energies with a resolution of 2.5% (5%) at 1 GeV in the barrel (end cap) region. The time resolution of the TOF barrel part is 68 ps, while that of the end cap part is 110 ps. More details about the design and performance of the BESIII detector are given in Ref. [10].

Simulated samples produced with GEANT4-based [13] Monte Carlo (MC) software, which includes the geometric description of the BESIII detector and the detector response, are used to determine the detection efficiency and to estimate background contributions. The simulations include the beam energy spread and initial state radiation in the e^+e^- annihilations modeled with the generator KKMC [14]. The inclusive MC samples consist of the production of $D\bar{D}$ pairs with quantum coherence (QC) for neutral D modes, the non-$D\bar{D}$ decays of the $\psi(3770)$, the initial state radiation production of the J/ψ and $\psi(3686)$ states, and the continuum processes. The known decay modes are modeled with EvtGen [15] using the branching fractions taken from the PDG [5], and the remaining unknown decays of the charmonium states are modeled by LUNDCHARM [16,17]. Final state radiation is incorporated using PHOTOS [18].

III. METHOD

As the peak of the $\psi(3770)$ resonance lies just above the $D\bar{D}$ threshold, it decays predominately into $D\bar{D}$ meson pairs. We take advantage of this by using a double-tag (DT) method, which was first developed by the MARKIII collaboration [19,20] to determine absolute branching fractions. The single-tag (ST) $\bar{D}^0(D^-)$ mesons are selected by using the two hadronic decay modes $\bar{D}^0 \to K^+\pi^-$ and $D^- \to K^+\pi^-\pi^-$, respectively, which have relatively large branching fractions and low background.

Events where $D^0(D^+)$ decaying into signal particles can be selected in the presence of ST $\bar{D}^0(D^-)$ mesons are called DT events. To compensate for the differences of the 3π invariant mass $M_{3\pi}$ distributions between data and MC simulation and to consider the signal migration among different $M_{3\pi}$ intervals, we determine the partial branching fractions of the $D^0(D^+) \to \pi^+\pi^+\pi^-X$ decays in bins of $M_{3\pi}$ at the production level. The numbers of produced DT events and the numbers of observed DT events are related in bins through a detector response matrix that accounts for detector efficiency and detector resolution,

$$N^i_{\rm obs} = \sum_{j=1}^{N_{\rm intervals}} \epsilon_{ij} N^j_{\rm prod}, \tag{1}$$

where $N^i_{\rm obs}$ is the number of signal events observed in the ith $M_{3\pi}$ interval, $N^j_{\rm prod}$ is the number of signal events produced in the jth $M_{3\pi}$ interval, and ϵ_{ij} is the efficiency matrix describing the detection efficiency and migration effect across each $M_{3\pi}$ interval. The statistical uncertainties of ϵ_{ij} due to the limited size of the signal MC simulation sample are considered as a source of systematic uncertainties, as discussed in Sec. VI.

The number of the inclusive decays $D^0(D^+) \to \pi^+\pi^+\pi^-X$ produced in the ith $M_{3\pi}$ interval is obtained by solving Eq. (1) for $N^i_{\rm prod}$, which gives

$$N^i_{\rm prod} = \sum_{j=1}^{N_{\rm intervals}} (\epsilon^{-1})_{ij} N^j_{\rm obs}. \tag{2}$$

The statistical uncertainty of $N^i_{\rm prod}$ is given by

$$(\sigma_{\rm stat}(N^i_{\rm prod}))^2 = \sum_{j=1}^{N_{\rm intervals}} (\epsilon^{-1})^2_{ij} (\sigma_{\rm stat}(N^j_{\rm obs}))^2, \tag{3}$$

where $\sigma_{\rm stat}(N^j_{\rm obs})$ is the statistical uncertainty of $N^j_{\rm obs}$.

The partial branching fraction of the ith $M_{3\pi}$ interval is determined by

$$\mathrm{d}\mathcal{B}_{\rm sig} = \frac{N^i_{\rm prod}}{N_{\rm ST}/\epsilon_{\rm tag}}, \tag{4}$$

where $N_{\rm ST}/\epsilon_{\rm tag}$ is the efficiency corrected yield of the ST $\bar{D}^0(D^-)$ mesons. The partial branching fractions are summed to obtain the total branching fraction $\mathcal{B}_{\rm sig}$.

Since the measurement of the branching fraction of $D^0 \to \pi^+\pi^+\pi^-X$ is affected by quantum coherence (QC) in the $D^0\bar{D}^0$ system, the branching fraction of

$D^0 \to \pi^+\pi^+\pi^- X$ measured with the tag mode $\bar{D}^0 \to K^+\pi^-$ needs to be corrected by

$$\mathrm{d}\mathcal{B}_{\mathrm{sig}}^{\mathrm{corr}} = f_{\mathrm{QC}}^{\mathrm{corr}} \times \mathrm{d}\mathcal{B}_{\mathrm{sig}}, \tag{5}$$

where

$$f_{\mathrm{QC}}^{\mathrm{corr}} = \frac{1}{1 - C_f(2f_{CP+} - 1)}, \tag{6}$$

$\mathrm{d}\mathcal{B}_{\mathrm{sig}}$ is the branching fraction to be measured, and C_f denotes the strong-phase factor calculated by

$$C_f = \frac{2rR\cos\delta}{1 + r^2}. \tag{7}$$

In Eq. (7), r is the ratio between the doubly-Cabibbo-suppressed and Cabibbo-favored amplitudes for $D \to K^\pm\pi^\mp$, δ is the strong phase difference between the two amplitudes and $R = 1$ is the coherence factor for $D \to K^\pm\pi^\mp$ [21,22]. Table I summarizes the parameters of r and δ for $D \to K^\pm\pi^\mp$, which give $C_f = (-11.3^{+0.4}_{-0.9})\%$ for $D \to K^\pm\pi^\mp$.

In Eq. (6), f_{CP+} is the fraction of the CP-even (+) component. According to Refs. [22,24], f_{CP+} is calculated by

$$f_{CP+} = \frac{N^+}{N^+ + N^-}$$

with

$$N^\pm = \frac{M^\pm_{\mathrm{measured}}}{S^\pm},$$

$$S_\pm = \frac{S^\pm_{\mathrm{measured}}}{1 - \eta_\pm y_D}.$$

Here, $N^\pm$ is the ratio of DT and ST yields with the CP-even and odd $CP \mp$ tags, $M^\pm_{\mathrm{measured}}$ denotes the number of DT candidates for a signal channel versus $CP \mp$ tags, and $S^\pm_{\mathrm{measured}}$ is the number of ST candidates for $CP\pm$ decay modes. Finally, $\eta_\pm = \pm 1$ for $CP\pm$ mode and $y_D = (0.62 \pm 0.08)\%$ is the mixing parameter of $D^0\bar{D}^0$ taken from the latest average by the PDG [5].

TABLE I. Input parameters for the QC correction.

Parameter	Value
$r_{K\pi}$	0.0586 ± 0.0002 [23]
$\delta_{K\pi}$	$(194.7^{+8.4}_{-17.0})^\circ$ [23]

IV. THE ST ANALYSIS

The charged kaons and pions are selected and identified with the same criteria as in Refs. [25,26]. For each charged track, the polar angle (θ) is required to be within the MDC acceptance $|\cos\theta| < 0.93$, where θ is defined with respect to the z axis, which is the symmetry axis of the MDC. The distance of the charged track's closest approach relative to the interaction point is required to be within 10 cm along the z axis and within 1 cm in the plane perpendicular to the z axis. Particle identification (PID) for charged tracks combines the measurements of $\mathrm{d}E/\mathrm{d}x$ in the MDC and the flight time in the TOF to form probabilities $\mathcal{L}(h)(h = K, \pi)$ for each hadron (h) hypothesis. Charged tracks are assigned as kaons or pions if their probabilities satisfy one of the two hypotheses, $\mathcal{L}(K) > \mathcal{L}(\pi)$ or $\mathcal{L}(\pi) > \mathcal{L}(K)$, respectively. In the selection of $\bar{D}^0 \to K^+\pi^-$ candidates, background contributions from cosmic rays and Bhabha events are rejected with the following requirements. First, the two charged tracks must have a TOF time difference less than 5 ns and they must not be consistent with being a muon pair or an electron-positron pair. Second, there must be at least one EMC shower with an energy greater than 50 MeV or at least one additional charged track detected in the MDC.

To distinguish the ST $\bar{D}$ mesons from combinatorial background, we define the two kinematic variables of energy difference ΔE and the beam-constrained mass M_{BC} as

$$\Delta E \equiv E_{\bar{D}} - E_{\mathrm{beam}}, \tag{8}$$

and

$$M_{\mathrm{BC}} \equiv \sqrt{E^2_{\mathrm{beam}}/c^4 - |\vec{p}_{\bar{D}}|^2/c^2}. \tag{9}$$

Here, E_{beam} is the beam energy, and $E_{\bar{D}}$ and $\vec{p}_{\bar{D}}$ are the energy and momentum of the $\bar{D}$ candidate in the rest frame of the e^+e^- system. For each ST mode, if there are multiple candidates in an event, the one with the least $|\Delta E|$ is kept. The ST $\bar{D}^0$ and D^- candidates are required to satisfy $|\Delta E| < 25$ and $|\Delta E| < 20$ MeV, respectively, which corresponds to about $\pm 3\sigma$ of the fitted resolution.

To determine the yields of ST $\bar{D}^0$ and D^- mesons, maximum likelihood fits are performed on the corresponding M_{BC} distributions of the accepted ST candidates. In the fits, the signal shape of $\bar{D}^0$ or D^- is modeled by an MC-simulated shape convolved with a double-Gaussian function, which is a sum of two Gaussian functions with free parameters, describing the resolution difference between data and MC simulation due to two asymmetrical tails of signal. The combinatorial background shape is described by an ARGUS function [27]. The resultant fits to the M_{BC} distributions are shown in Fig. 1. The yields of ST $\bar{D}^0$ and D^- mesons are 548031 ± 775 and 812109 ± 1896, respectively, where the uncertainties are statistical only. The efficiencies of reconstructing the ST $\bar{D}$ mesons are

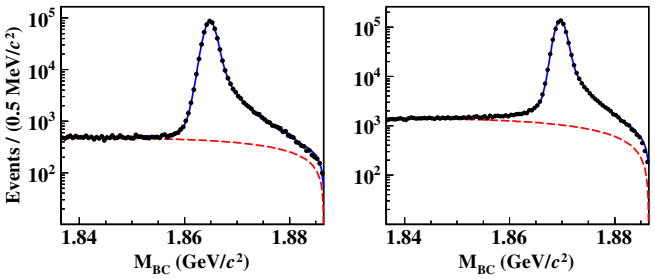

FIG. 1. Fits to the $M_{\rm BC}$ distributions of the ST candidates for $\bar{D}^0 \to K^+\pi^-$ (left) and $D^- \to K^+\pi^-\pi^-$ (right), where the points with error bars are data, the blue solid curves are the fit results, and the red dashed curves are the fitted combinatorial backgrounds.

estimated to be $(67.70 \pm 0.08)\%$ and $(51.58 \pm 0.04)\%$ for neutral $\bar{D}^0$ decay and charged D^- decay, respectively, by analyzing the inclusive MC sample with the same procedure as that for data.

V. THE DT ANALYSIS

A. Selection of $D^0(D^+) \to \pi^+\pi^+\pi^-X$

The candidates for $D^0(D^+) \to \pi^+\pi^+\pi^-X$ are selected in the presence of the ST $\bar{D}$ mesons. We require that there are at least three charged pions which have not been used in the ST selection. If there are more than one π^- or two π^+ mesons reconstructed on the signal side, only the one with the fastest two π^+s and the fastest π^- are kept for further analysis.

To reject background components from $D^0(D^+) \to \pi^+K^0_S(\to \pi^+\pi^-)X$ decays (K^0_S BKG1), the invariant mass of any $\pi^+\pi^-$ combination from the three selected pions is required to fulfill $|M_{\pi^+\pi^-} - 0.4977| > 0.030$ GeV/c^2. Here, there is no decay length requirement for K^0_S BKG1. In addition, another K^0_S background (K^0_S BKG2), where one of the π mesons comes from the chosen three pions and another assumed π meson comes from a remaining oppositely charged track without PID, is rejected. The K^0_S candidate is selected through the following selection criteria: First, the $\pi^+\pi^-$ pair is constrained to originate from a common vertex. Second, the invariant mass of the $\pi^+\pi^-$ pair is in the range of $|M_{\pi^+\pi^-} - 0.4977| > 0.012$ GeV/c^2. Third, the decay length of K^0_S candidate is greater than 2 standard deviations of the vertex resolution away from the interaction point.

To further suppress the remaining background contributions of K^0_S BKG2 and $D^0 \to \pi^+\pi^-K^0_S(\to \pi^+\pi^-)$ (K^0_S BKG3), the recoil masses of the $\bar{D}^0\pi^+\pi^-$ combinations are required to be $|M_{\pi^+\pi^-} - 0.4977| > 0.080$ GeV/c^2. For background contributions from $D^0 \to \pi^+\pi^-\pi^0K^0_S$ (K^0_S BKG3), a similar requirement is applied on $\bar{D}^0\pi^+\pi^-\pi^0$ combinations if a good π^0 is found. The π^0 candidates are reconstructed via the $\pi^0 \to \gamma\gamma$ decay and the opening angle between the photon candidate and the nearest charged track is required to be greater than 10°. Any photon pair with an invariant mass between $(0.115, 0.150)$ GeV/c^2 is regarded as a π^0 candidate, and a kinematic fit is imposed on the photon pair to constrain its invariant mass to the known π^0 mass [5].

Figure 2 shows the comparison of the distributions of $M_{3\pi}$ and $M_{\rm miss}$ of the selected charged pions for the accepted DT candidates between data and the inclusive MC sample. Throughout this paper, $M_{3\pi}$ is the invariant mass of the selected $\pi^+\pi^+\pi^-$ combination and $M_{\rm miss}$ is the missing mass of the $\bar{D}\pi^+\pi^+\pi^-$ combination given by

$$M^2_{\rm miss} = (2E_{\rm beam} - E_{\bar{D}} - E_{3\pi})^2/c^4 - |-\vec{p}_{\bar{D}} - \vec{p}_{3\pi}|^2/c^2, \tag{10}$$

where $E_{3\pi}$ and $\vec{p}_{3\pi}$ are the total energy and momentum of the selected $\pi^+\pi^+\pi^-$ combination of the signal side in the e^+e^- center-of-mass frame. Small inconsistencies between data and the inclusive MC sample around $(0.9, 1.2)$ GeV/c^2 in the $M_{3\pi}$ distributions are mainly due to imperfect simulations of multibody hadronic decays with low branching fractions. For the $D^0 \to \pi^+\pi^+\pi^-X$ and $D^+ \to \pi^+\pi^+\pi^-X$ decays, the largest signal components are from $D^0 \to K^-\pi^+\pi^+\pi^-$ and $D^+ \to \bar{K}^0\pi^+\pi^+\pi^-$ decays, respectively, and they form peaks around the known $\bar{K}$ mass in the $M_{\rm miss}$ distributions as expected. For $D^+ \to \pi^+\pi^+\pi^-X$, the peak around the known D^+ mass in the $M_{3\pi}$ distribution is from $D^+ \to \pi^+\pi^+\pi^-$; the peaks around zero and 0.135 GeV/c^2 in the $M_{\rm miss}$ distribution are from $D^+ \to \pi^+\pi^+\pi^-$ and $D^+ \to \pi^+\pi^+\pi^-\pi^0$, respectively; the peak around 0.548 GeV/c^2 in the $M_{\rm miss}$ distribution is mainly from $D^+ \to \pi^+\pi^+\pi^-\eta$. Comparisons of the distributions of

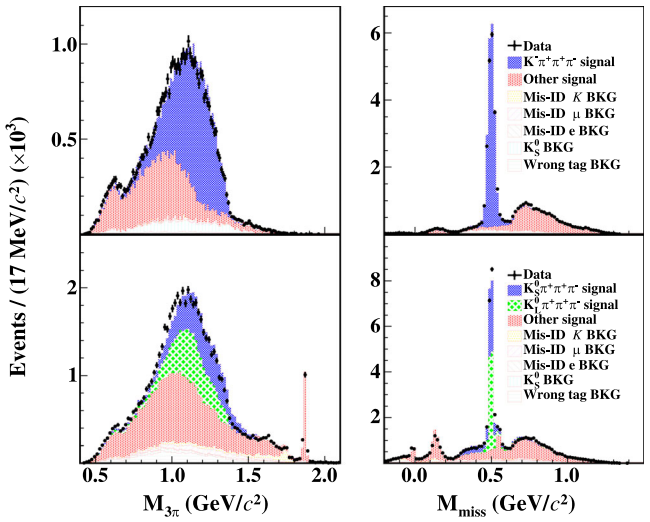

FIG. 2. Comparisons of the $M_{3\pi}$ (left) and $M_{\rm miss}$ (right) distributions of the DT candidates for $D^0 \to \pi^+\pi^+\pi^-X$ (top) and $D^+ \to \pi^+\pi^+\pi^-X$ (bottom), where the points with error bars are data and the color filled histograms are the inclusive MC sample. To ensure a $\bar{D}$ in the ST side, events must satisfy the requirements mentioned in the text and an additional requirement of $|M_{\rm BC} - M_D| < 0.005$ GeV/c^2, where M_D is the known D mass [5].

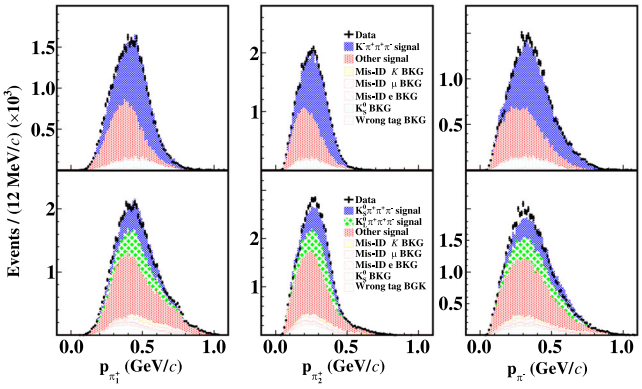

FIG. 3. Comparisons of the momentum distributions of the selected pions of the DT candidates for $D^0 \to \pi^+\pi^+\pi^-X$ (top) and $D^+ \to \pi^+\pi^+\pi^-X$ (bottom), where the points with error bars are data and the color filled histograms are the inclusive MC sample. To ensure a $\bar{D}$ in the ST side, events must satisfy the requirements mentioned in the text and an additional requirement of $|M_{\rm BC} - M_D| < 0.005$ GeV/c^2, where M_D is the known D mass [5], and π_1^+ and π_2^+ denote the higher and lower momentum π^+s, respectively.

momenta of the selected three charged pions are in good agreement, as shown in Fig. 3.

Background analysis based on the inclusive MC sample shows that there are still some remaining background components, even after imposing all the aforementioned background rejection requirements. One is from eventswith wrongly tagged $\bar{D}$ decays (i.e. ST decays are not $\bar{D}^0 \to K^+\pi^-$ or $D^- \to K^+\pi^-\pi^-$) and the non-$D\bar{D}$ process, labeled as "wrong tag." Another background component results from events with correctly tagged $\bar{D}$ decays, but incorporating particle misidentifications of $K \to \pi$ (Mis-ID K BKG), $\mu \to \pi$ (Mis-ID μ BKG) and $e \to \pi$ (Mis-ID e BKG) as well as the remaining K^0_S background (K^0_S BKG). The background components are also shown in Figs. 2 and 3.

B. DT signal yields

To minimize a possible efficiency dependence of various D decay modes and offer finer information for the LFU tests in the semileptonic B decays, the partial branching fractions of $D^0 \to \pi^+\pi^+\pi^-X$ and $D^+ \to \pi^+\pi^+\pi^-X$ are measured in nine and ten $M_{3\pi}$ bins, respectively. For $D^0 \to \pi^+\pi^+\pi^-X$ and $D^+ \to \pi^+\pi^+\pi^-X$, the lower boundaries of the intervals are chosen as $[0.40, 0.55, 0.70, 0.85, 1.00, 1.15, 1.30, 1.45, 1.60, 1.75]$ GeV/c^2 and $[0.40, 0.55, 0.70, 0.85, 1.00, 1.15, 1.30, 1.45, 1.60, 1.75, 2.00]$ GeV/c^2, respectively. For $D^+ \to \pi^+\pi^+\pi^-X$, the interval $[1.75, 2.00]$ GeV/c^2 is added to specifically consider the hadronic decay $D^+ \to \pi^+\pi^+\pi^-$.

The signal yields in each $M_{3\pi}$ bin are determined by fitting the $M_{\rm BC}$ distributions of the ST side when the candidates for $D^0 \to \pi^+\pi^+\pi^-X$ and $D^+ \to \pi^+\pi^+\pi^-X$ are found. Figures 4(a) and 4(b) show the $M_{\rm BC}$ distributions of the accepted candidates for $D^0 \to \pi^+\pi^+\pi^-X$ and

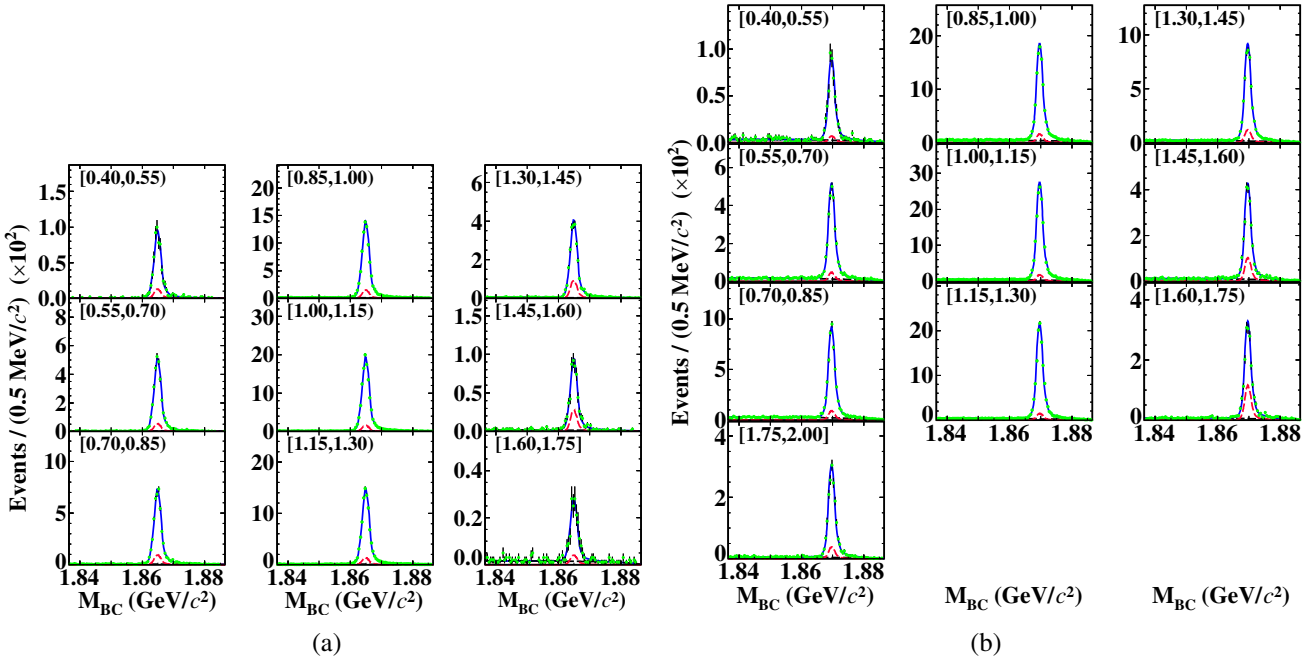

FIG. 4. Fits to the $M_{\rm BC}$ distributions of the tag side when the candidates for (a) $D^0 \to \pi^+\pi^+\pi^-X$ and (b) $D^+ \to \pi^+\pi^+\pi^-X$ are found in various reconstructed $M_{3\pi}$ intervals (in unit of GeV/c^2) indicated on each plot. The points with error bars are data, the blue solid curves are the fit results, the pink dashed curves are the peaking background summing over Mis-ID K BKG, Mis-ID μ BKG, Mis-ID e BKG, and K^0_S BKG, and the black dashed curves are the fitted combinatorial backgrounds.

TABLE II. Signal yields ($N_{\rm obs}$) of $D^0 \to \pi^+\pi^+\pi^-X$ observed from data in various reconstructed $M_{3\pi}$ intervals. The numbers of background events are estimated by the inclusive MC sample, whose integrated luminosity is 4 times that of data. The uncertainties of $N_{\rm Mis-ID\,\mathit{K}\,BKG}$, $N_{\rm Mis-ID\,\mu\,BKG}$, $N_{\rm Mis-ID\,\mathit{e}\,BKG}$, and $N_{K^0_S\,\rm BKG}$ include statistical uncertainties and the uncertainties of individual differences of the particle misidentification rates between data and MC simulation. The uncertainties of $N_{\rm obs}$ are statistical only.

$M_{3\pi}$ (GeV/c^2)	$N_{\rm Mis-ID\,\mathit{K}\,BKG}$	$N_{\rm Mis-ID\,\mu\,BKG}$	$N_{\rm Mis-ID\,\mathit{e}\,BKG}$	$N_{K^0_S\,\rm BKG}$	$N_{\rm obs}$
[0.40, 0.55)	29.1 ± 6.9	0.0 ± 0.0	4.7 ± 0.9	45.5 ± 3.5	524.4 ± 24.8
[0.55, 0.70)	78.1 ± 15.8	3.1 ± 1.0	26.7 ± 2.3	221.0 ± 7.8	2878.7 ± 57.3
[0.70, 0.85)	81.5 ± 14.7	21.2 ± 2.6	32.8 ± 2.8	428.1 ± 10.8	4017.2 ± 69.6
[0.85, 1.00)	85.9 ± 14.3	73.8 ± 4.8	43.2 ± 3.4	721.4 ± 14.1	7824.8 ± 96.0
[1.00, 1.15)	58.8 ± 9.4	127.6 ± 6.3	35.3 ± 3.2	766.6 ± 14.5	11221.3 ± 111.9
[1.15, 1.30)	13.8 ± 2.9	99.3 ± 5.4	21.3 ± 2.5	670.2 ± 13.5	8540.3 ± 98.8
[1.30, 1.45)	15.0 ± 2.9	49.4 ± 3.8	11.2 ± 1.9	485.0 ± 11.5	1966.5 ± 51.8
[1.45, 1.60)	6.4 ± 1.6	17.6 ± 2.2	6.2 ± 1.4	135.3 ± 6.1	417.7 ± 25.3
[1.60, 1.75]	2.8 ± 1.0	0.6 ± 0.4	0.0 ± 0.0	21.1 ± 2.4	145.9 ± 14.3

$D^+ \to \pi^+\pi^+\pi^-X$. The fits to these $M_{\rm BC}$ distributions are similar to those of the ST side. Because the wrong tag background events do not form peaking background in the $M_{\rm BC}$ distribution of the tag side, an ARGUS function is used to describe the wrong tag background. In these fits, however, the parameters of the Gaussian functions and the ARGUS functions are fixed to the values from the $M_{\rm BC}$ fits of the ST side. In addition, since the Mis-ID K BKG, Mis-ID μ BKG, Mis-ID e BKG, and K^0_S BKG components can peak in the distribution of $M_{\rm BC}$, the contributions of those backgrounds must be subtracted. The yields and shapes of the Mis-ID K BKG, Mis-ID μ BKG, Mis-ID e BKG, and K^0_S BKG components are fixed based on the fits to the $M_{\rm BC}$ distributions of the background events from the inclusive MC sample, after taking into account the differences of the rates of misidentifying various particles as charged pions between data and MC simulation. The fixed background yields and the signal yields in various $M_{3\pi}$ intervals for $D^0 \to \pi^+\pi^+\pi^-X$ and $D^+ \to \pi^+\pi^+\pi^-X$ are summarized in Tables II and III, respectively.

The efficiency matrix $\epsilon_{ij} = N^{ij}_{\rm reco}/N^{j}_{\rm prod}$ is determined based on signal MC events of all known exclusive $D^{0(+)}$ decays that contain a $\pi^+\pi^+\pi^-$ combination, where $N^{ij}_{\rm reco}$ is the number of signal MC events generated in the jth $M_{3\pi}$ interval and reconstructed in the ith interval. The matrix elements of ϵ_{ij} for $D^0 \to \pi^+\pi^+\pi^-X$ and $D^+ \to \pi^+\pi^+\pi^-X$ are summarized in Tables IV and V, respectively.

C. Branching fractions

With the obtained yields of the inclusive decays $D^0(D^+) \to \pi^+\pi^+\pi^-X$ produced in the ith $M_{3\pi}$ interval, the partial decay branching fraction is determined by Eq. (4).

The measurement of the branching fraction of $D^0 \to \pi^+\pi^+\pi^-X$ is affected by the QC effect in neutral D decays, as discussed in Sec. III. In this work, the QC factors in the various $M_{3\pi}$ intervals are estimated by using the CP-even (+) tag of $D^0 \to K^+K^-$ and CP-odd (−) tag of $D^0 \to K^0_S\pi^0$ with a similar analysis procedure as the one in the data

TABLE III. Signal yields ($N_{\rm obs}$) of $D^+ \to \pi^+\pi^+\pi^-X$ observed from data in various reconstructed $M_{3\pi}$ intervals. The numbers of background events are estimated by the inclusive MC sample, whose integrated luminosity is 4 times that of data. The uncertainties of $N_{\rm Mis-ID\,\mathit{K}\,BKG}$, $N_{\rm Mis-ID\,\mu\,BKG}$, $N_{\rm Mis-ID\,\mathit{e}\,BKG}$, and $N_{K^0_S\,\rm BKG}$ include statistical uncertainties and the uncertainties of individual differences of the particle misidentification rates between data and MC simulation. The uncertainties of $N_{\rm obs}$ are statistical only.

$M_{3\pi}$ (GeV/c^2)	$N_{\rm Mis-ID\,\mathit{K}\,BKG}$	$N_{\rm Mis-ID\,\mu\,BKG}$	$N_{\rm Mis-ID\,\mathit{e}\,BKG}$	$N_{K^0_S\,\rm BKG}$	$N_{\rm obs}$
[0.40, 0.55)	21.6 ± 4.5	4.5 ± 0.9	6.0 ± 0.9	9.7 ± 1.2	483.3 ± 24.5
[0.55, 0.70)	126.1 ± 20.6	52.4 ± 3.2	29.6 ± 1.9	76.2 ± 3.5	2703.8 ± 58.4
[0.70, 0.85)	254.3 ± 37.4	119.6 ± 4.9	42.4 ± 2.5	127.7 ± 4.5	4766.7 ± 77.6
[0.85, 1.00)	506.6 ± 66.7	244.4 ± 7.1	57.4 ± 3.1	151.6 ± 4.9	9788.2 ± 109.6
[1.00, 1.15)	535.4 ± 61.0	346.7 ± 8.2	75.2 ± 3.6	131.3 ± 4.6	14979.8 ± 132.3
[1.15, 1.30)	365.1 ± 35.8	365.4 ± 8.2	36.1 ± 2.6	123.6 ± 4.5	11718.5 ± 117.0
[1.30, 1.45)	292.4 ± 25.8	296.1 ± 7.2	16.0 ± 1.7	107.3 ± 4.2	4636.0 ± 76.8
[1.45, 1.60)	320.4 ± 24.6	195.2 ± 5.8	6.6 ± 1.1	91.0 ± 3.8	1864.6 ± 52.8
[1.60, 1.75)	557.3 ± 34.8	84.4 ± 3.7	3.0 ± 0.7	47.5 ± 2.8	1228.0 ± 46.0
[1.75, 2.00]	157.4 ± 12.1	15.5 ± 1.6	0.6 ± 0.3	57.0 ± 3.0	1559.3 ± 44.1

TABLE IV. Efficiency matrix ϵ_{ij} (in percent) for $D^0 \to \pi^+\pi^+\pi^-X$, where i denotes the reconstructed $M_{3\pi}$ interval and j denotes the produced $M_{3\pi}$ interval. The relative statistical uncertainties of the diagonal efficiencies of the matrix are no more than 0.7%.

ϵ_{ij}	1	2	3	4	5	6	7	8	9
1	27.74	0.79	0.08	0.03	0.00	0.01	0.03	0.00	0.00
2	2.82	27.99	1.01	0.24	0.06	0.02	0.03	0.08	0.00
3	0.70	0.95	25.70	0.90	0.16	0.05	0.12	0.34	0.27
4	0.69	0.62	0.96	32.65	1.27	0.25	0.20	0.65	0.54
5	0.44	0.45	0.33	1.25	42.40	2.07	0.78	0.98	0.54
6	0.13	0.09	0.11	0.20	1.07	47.82	3.21	0.81	0.00
7	0.00	0.05	0.03	0.06	0.14	0.90	40.78	1.74	0.54
8	0.00	0.00	0.00	0.01	0.01	0.05	0.28	22.28	0.80
9	0.00	0.00	0.00	0.00	0.00	0.01	0.00	0.34	20.57

TABLE V. Efficiency matrix ϵ_{ij} (in percent) for $D^+ \to \pi^+\pi^+\pi^-X$, where i denotes the reconstructed $M_{3\pi}$ interval and j denotes the produced $M_{3\pi}$ interval. The relative statistical uncertainties of the diagonal efficiencies of the matrix are no more than 0.5%.

ϵ_{ij}	1	2	3	4	5	6	7	8	9	10
1	22.13	0.48	0.11	0.04	0.03	0.03	0.02	0.01	0.00	0.00
2	2.18	24.02	0.99	0.25	0.18	0.13	0.11	0.08	0.01	0.00
3	0.99	1.71	22.44	1.30	0.41	0.25	0.29	0.10	0.00	0.01
4	0.90	1.24	1.90	30.31	2.14	0.83	0.66	0.13	0.04	0.01
5	0.81	1.01	1.49	2.53	39.52	3.35	1.33	0.27	0.03	0.01
6	0.47	0.71	1.03	1.65	3.39	47.30	3.87	0.35	0.04	0.00
7	0.46	0.50	0.75	1.27	1.99	2.33	50.08	2.14	0.34	0.03
8	0.15	0.22	0.23	0.36	0.38	0.18	0.76	54.16	2.29	0.19
9	0.00	0.00	0.00	0.00	0.01	0.01	0.03	1.28	56.79	1.18
10	0.02	0.00	0.00	0.00	0.00	0.00	0.01	0.05	0.71	55.00

analysis procedure presented above. The quantities used and the results are summarized in Table VI.

The produced signal yields and the obtained partial branching fractions of $D^0 \to \pi^+\pi^+\pi^-X$ and $D^+ \to \pi^+\pi^+\pi^-X$ in different $M_{3\pi}$ intervals are presented in Tables VII and VIII, respectively.

VI. SYSTEMATIC UNCERTAINTIES

Benefiting from the DT method, the branching fraction measurements are insensitive to the selection criteria of the ST $\bar{D}$ candidates. The systematic uncertainties in the measurements of the branching fractions of $D^0 \to \pi^+\pi^+\pi^-X$ and $D^+ \to \pi^+\pi^+\pi^-X$ are discussed below.

Both the ST and DT yields are determined from the fits to the individual $M_{\rm BC}$ distributions. The fits to the DT candidates are performed by using the same fit strategy as the fits to the ST candidates, with the parameters of the smeared Gaussian function and the ARGUS background function derived from the corresponding fits to the ST candidates. In this case, the fitted DT yields are correlated to those of the fitted ST yields. Therefore, the systematic

TABLE VI. Quantities of $S^{\pm}_{\rm measured}$, $M^{\pm}_{\rm measured}$, C_f, f_{CP+} and $f^{\rm corr}_{\rm QC}$ for $D^0 \to \pi^+\pi^+\pi^-X$ in various reconstructed $M_{3\pi}$ intervals.

i	$S^-_{\rm measured}$	$S^+_{\rm measured}$	C_f (%)	$M^-_{\rm measured}$	$M^+_{\rm measured}$	f_{CP+}	$f^{\rm corr}_{\rm QC}$
1				171.8 ± 41.6	161.9 ± 46.0	0.46 ± 0.14	1.01 ± 0.03
2				1163.4 ± 90.3	857.1 ± 84.6	0.53 ± 0.05	0.99 ± 0.01
3				1729.7 ± 224.1	2124.3 ± 481.8	0.40 ± 0.08	1.02 ± 0.02
4				2697.6 ± 149.4	2620.2 ± 295.8	0.46 ± 0.04	1.01 ± 0.01
5	70999 ± 304	59238 ± 442	$-11.3^{+0.4}_{-0.9}$	3241.0 ± 132.0	2798.1 ± 161.7	0.49 ± 0.03	1.00 ± 0.01
6				1776.2 ± 79.6	2108.6 ± 89.8	0.41 ± 0.02	1.02 ± 0.01
7				360.7 ± 52.2	547.9 ± 72.6	0.35 ± 0.10	1.04 ± 0.03
8				250.2 ± 50.5	186.0 ± 45.6	0.52 ± 0.18	0.99 ± 0.04
9				121.8 ± 33.8	21.5 ± 8.1	0.82 ± 0.60	0.93 ± 0.12

TABLE VII. The produced signal yields and the obtained partial branching fractions of $D^0 \to \pi^+\pi^+\pi^-X$ in different reconstructed $M_{3\pi}$ intervals. $d\mathcal{B}^{CP}_{\rm sig}$ is the partial decay branching fraction corrected by the QC factor, where $d\mathcal{B}^{\rm corr}_{\rm sig} = f^{\rm corr}_{\rm QC} \times d\mathcal{B}_{\rm sig}$ according to Eq. (5).

i	$N_{\rm prod}$	$d\mathcal{B}_{\rm sig}$	$d\mathcal{B}^{\rm corr}_{\rm sig}$ (%)
1	1541.3 ± 89.9	0.28 ± 0.02	0.28 ± 0.02
2	9349.1 ± 206.0	1.71 ± 0.04	1.70 ± 0.04
3	14235.8 ± 271.8	2.60 ± 0.05	2.66 ± 0.05
4	22130.5 ± 295.0	4.04 ± 0.05	4.08 ± 0.05
5	24638.2 ± 264.9	4.50 ± 0.05	4.51 ± 0.05
6	16850.4 ± 207.4	3.07 ± 0.04	3.14 ± 0.04
7	4228.6 ± 127.5	0.77 ± 0.02	0.80 ± 0.02
8	1730.9 ± 113.7	0.32 ± 0.02	0.31 ± 0.02
9	676.1 ± 69.6	0.12 ± 0.01	0.11 ± 0.01
Total	95381.0 ± 598.9	⋯	17.60 ± 0.11

TABLE VIII. The produced signal yields and the obtained partial branching fractions of $D^+ \to \pi^+\pi^+\pi^-X$ in different reconstructed $M_{3\pi}$ intervals.

i	$N_{\rm prod}$	$d\mathcal{B}_{\rm sig}$ (%)
1	1747.1 ± 111.1	0.22 ± 0.01
2	9683.3 ± 245.1	1.19 ± 0.03
3	17890.3 ± 349.6	2.20 ± 0.04
4	27671.6 ± 366.3	3.41 ± 0.05
5	33224.6 ± 340.2	4.09 ± 0.04
6	20383.9 ± 251.5	2.51 ± 0.03
7	5772.7 ± 155.4	0.71 ± 0.02
8	2661.8 ± 97.8	0.33 ± 0.01
9	2032.0 ± 81.1	0.25 ± 0.01
10	2803.0 ± 80.2	0.35 ± 0.01
Total	123870.2 ± 744.7	15.25 ± 0.09

uncertainties in the yields of the ST $\bar{D}$ mesons are canceled in the branching fraction measurements.

The tracking and PID efficiencies of $\pi^\pm$ are studied with the DT hadronic $D\bar{D}$ events. The averaged data/MC differences of $\pi^\pm$ tracking and PID efficiencies, weighted by the corresponding momentum spectra of signal MC events, are 0.62% and 0.17%, respectively. After correcting the MC efficiencies to data by these averaged data/MC differences, the systematic uncertainties of tracking and PID efficiencies for the three charged pions are assigned as 0.80% and 0.50% for $D^0 \to \pi^+\pi^+\pi^-X$ and $D^+ \to \pi^+\pi^+\pi^-X$, respectively.

The detection efficiencies of $D^{0(+)} \to \pi^+\pi^+\pi^-X$ are obtained from the signal MC sample including all known decays with three charged pions. The relevant systematic uncertainties are estimated by varying the input branching fractions of exclusive decays within $\pm 1\sigma$. The maximum changes of the detection efficiencies, 0.13% and 0.56%, are assigned as the corresponding systematic uncertainties for $D^0 \to \pi^+\pi^+\pi^-X$ and $D^+ \to \pi^+\pi^+\pi^-X$, respectively.

The uncertainties due to the limited signal DT MC samples are calculated by [28]

$$C^{\rm sys}_{ij} = \left(\frac{1}{N_{\rm ST}}\right)^2 \sum_{\alpha\beta} N^{\alpha}_{\rm obs} N^{\beta}_{\rm obs} {\rm Cov}(\epsilon^{-1}_{i\alpha}, \epsilon^{-1}_{j\beta}), \quad (11)$$

where the covariances of the inverse efficiency matrix elements are given by

$$ {\rm Cov}(\epsilon^{-1}_{\alpha\beta}, \epsilon^{-1}_{ab}) = \sum_{ij} (\epsilon^{-1}_{\alpha i}\epsilon^{-1}_{ai})[\sigma(\epsilon_{ij})]^2(\epsilon^{-1}_{j\beta}\epsilon^{-1}_{jb}). \quad (12)$$

The corresponding systematic uncertainties are assigned to be 0.31% and 0.23% for $D^0 \to \pi^+\pi^+\pi^-X$ and $D^+ \to \pi^+\pi^+\pi^-X$, respectively.

The efficiencies of misidentifying $e^\pm$, $\mu^\pm$ and $K^\pm$ as $\pi^\pm$ are studied with the $e^+e^- \to \gamma e^+e^-$ events, the $e^+e^- \to \gamma\mu^+\mu^-$ events, and the DT hadron $D\bar{D}$ events, respectively. The averaged data/MC differences of the efficiencies of misidentifying $e^\pm$ ($\mu^\pm$) as $\pi^\pm$, weighted by the two-dimensional (momentum and $\cos\theta$) distributions of signal MC events, are 12% and 5%, respectively. The averaged data/MC differences of the efficiencies of misidentifying $K^\pm$ as $\pi^\pm$, weighted by the corresponding momentum spectra of signal MC events, are no more than 53%. Here, the large data/MC differences in some $M_{3\pi}$ intervals are mainly due to extremely small rates of misidentifying $K^\pm$ as $\pi^\pm$, which are in the range of (0.05–0.72)% for $p_K < 0.7$ GeV/c. After correcting these misidentification efficiencies to data by these averaged data/MC differences, the associated systematic uncertainties are estimated by varying the fixed background yields within their individual uncertainties. Their effects on the measured branching fractions are 0.13% and 0.18% for $D^0 \to \pi^+\pi^+\pi^-X$ and $D^+ \to \pi^+\pi^+\pi^-X$, respectively.

The yields of background with correct $\bar{D}$ tag but wrong D signal are estimated using the inclusive MC sample. The relevant systematic uncertainty is evaluated by varying the world average branching fractions of the top five background components (which account for more than 52% of all background contributions) of the decays in $D^{0(+)} \to \pi^+\pi^+\pi^-X$ within $\pm 1\sigma$. The changes of the branching fractions are assigned as the corresponding systematic uncertainties, which are 0.09% and 0.20% for $D^0 \to \pi^+\pi^+\pi^-X$ and $D^+ \to \pi^+\pi^+\pi^-X$, respectively. The effects of the remaining background components are also examined similarly and found to be negligible.

The K^0_S veto is considered in three aspects. The first systematic uncertainty comes from the requirements of rejecting (K^0_S BKG1). The associated systematic uncertainty is estimated by altering the nominal veto window of

$|M_{\pi^+\pi^-} - 0.4977| > 0.030$ GeV/c^2 by ± 5 MeV/c^2, which corresponds to about 1σ of the fitted K_S^0 mass resolution. The largest change of the remeasured branching fraction is taken as the systematic uncertainties, which are 0.23% and 0.06% for $D^0 \to \pi^+\pi^+\pi^-X$ and $D^+ \to \pi^+\pi^+\pi^-X$, respectively. The second systematic uncertainty comes from the requirements of rejecting (K_S^0 BKG2), and it is estimated by varying the background yields by $\pm 1.5\%$ in the $M_{\rm BC}$ fit. Here, the 1.5% corresponds to the data/MC difference of the K_S^0 reconstruction efficiencies between data and MC simulation, estimated with the control samples of $J/\psi \to K^*(892)^\mp K^\pm$ and $J/\psi \to \phi K_S^0 K^\pm \pi^\mp$ [29]. The changes in the remeasured branching fractions are assigned as the systematic uncertainties, which are 0.11% and 0.17% for $D^0 \to \pi^+\pi^+\pi^-X$ and $D^+ \to \pi^+\pi^+\pi^-X$, respectively. The third systematic uncertainty comes from the requirements of rejecting (K_S^0 BKG3), and it is estimated by altering the nominal veto window of $|M_{\pi^+\pi^-} - 0.4977| > 0.080$ GeV/c^2 by ± 5 MeV/c^2. The largest change of the remeasured branching fraction is taken as the systematic uncertainty, which is 0.28% for $D^0 \to \pi^+\pi^+\pi^-X$. Adding these three items in quadrature yields the systematic uncertainties due to K_S^0 veto to be 0.38% and 0.18% for $D^0 \to \pi^+\pi^+\pi^-X$ and $D^+ \to \pi^+\pi^+\pi^-X$, respectively.

The systematic uncertainties due to $M_{3\pi}$ divisions are estimated by increasing or decreasing the interval number by 50%. The larger differences of the remeasured branching fractions to the nominal results are assigned as the systematic uncertainties, which are 0.34% and 0.20% for $D^0 \to \pi^+\pi^+\pi^-X$ and $D^+ \to \pi^+\pi^+\pi^-X$, respectively.

The systematic uncertainty due to the correction factor of QC effect in $D^0 \to \pi^+\pi^+\pi^-X$ decays is determined by the residual uncertainty of $f_{\rm QC}^{\rm corr}$, which are summarized in Table VI. After weighting by the corresponding numbers of the inclusive decays $D^0 \to \pi^+\pi^+\pi^-X$ produced in each $M_{3\pi}$ interval, 0.42% is taken as the systematic uncertainty.

TABLE IX. Relative systematic uncertainties (in percent) in the measurements of the branching fractions of $D^0 \to \pi^+\pi^+\pi^-X$ and $D^+ \to \pi^+\pi^+\pi^-X$.

Source	$D^0 \to \pi^+\pi^+\pi^-X$	$D^+ \to \pi^+\pi^+\pi^-X$
$\pi^\pm$ tracking	0.80	0.80
$\pi^\pm$ PID	0.50	0.50
Efficiency estimate	0.13	0.56
MC statistics	0.31	0.23
Misidentification efficiencies	0.13	0.18
Background estimate	0.09	0.20
K_S^0 vetoes	0.38	0.18
QC correction factor	0.42	...
Binning scheme	0.34	0.20
Total	1.23	1.18

Assuming all systematic uncertainties to be uncorrelated and adding them in quadrature, we obtain the total systematic uncertainties in the measurements of the branching fractions of $D^0 \to \pi^+\pi^+\pi^-X$ and $D^+ \to \pi^+\pi^+\pi^-X$ to be 1.23% and 1.18%, respectively. Table IX summarizes the systematic uncertainties discussed above.

VII. SUMMARY

By analyzing 2.93 fb^{-1} of e^+e^- collision data taken at $\sqrt{s} = 3.773$ GeV, we have measured the branching fractions of the inclusive decays $D^0 \to \pi^+\pi^+\pi^-X$ and $D^+ \to \pi^+\pi^+\pi^-X$ for the first time. The results are

$$\mathcal{B}(D^0 \to \pi^+\pi^+\pi^-X) = (17.60 \pm 0.11 \pm 0.22)\%,$$

and

$$\mathcal{B}(D^+ \to \pi^+\pi^+\pi^-X) = (15.25 \pm 0.09 \pm 0.18)\%,$$

where the first uncertainties are statistical and the second are systematic. They are consistent with the sums of the branching fractions of the known decay modes as summarized in the Appendix within about $\pm 3\sigma$. The partial branching fraction in the interval $[1.75, 2.00]$ GeV/c^2 is consistent with the branching fraction of the exclusive hadronic decay of $D^+ \to \pi^+\pi^+\pi^-$, which is $(0.327 \pm 0.018)\%$ according to the PDG [5]. These results indicate that there is little room for possible missing $D^0(D^+)$ decays containing $\pi^+\pi^+\pi^-$. The measured total and partial branching fractions of $D^0(D^+) \to \pi^+\pi^+\pi^-X$ are important inputs for LFU tests for the semileptonic B decays.

ACKNOWLEDGMENTS

The BESIII collaboration thanks the staff of BEPCII and the Institute of High Energy Physics (IHEP) computing center for their strong support. This work is supported in part by National Key R&D Program of China under Grants No. 2020YFA0406400 and No. 2020YFA0406300; National Natural Science Foundation of China (NSFC) under Grants No. 11875170, No. 12035009, No. 11635010, No. 11735014, No. 11835012, No. 11935015, No. 11935016, No. 11935018, No. 11961141012, No. 12022510, No. 12025502, No. 12035013, No. 12061131003, No. 12192260, No. 12192261, No. 12192262, No. 12192263, No. 12192264, and No. 12192265; the Chinese Academy of Sciences (CAS) Large-Scale Scientific Facility Program; the CAS Center for Excellence in Particle Physics (CCEPP); Joint Large-Scale Scientific Facility Funds of the NSFC and CAS under Grant No. U1832207; CAS Key Research Program of Frontier Sciences under Grants No. QYZDJ-SSW-SLH003 and No. QYZDJ-SSW-SLH040; 100 Talents Program of CAS; The Institute of Nuclear and Particle Physics (INPAC) and Shanghai Key Laboratory for Particle

Physics and Cosmology; ERC under Grant No. 758462; European Union's Horizon 2020 research and innovation program under Marie Sklodowska-Curie grant agreement under Grant No. 894790; German Research Foundation DFG under Grants No. 443159800 and No. 455635585, Collaborative Research Center CRC 1044, FOR5327, GRK 2149; Istituto Nazionale di Fisica Nucleare, Italy; Ministry of Development of Turkey under Grant No. DPT2006K-120470; National Science and Technology fund; National Science Research and Innovation Fund (NSRF) via the Program Management Unit for Human Resources & Institutional Development, Research and Innovation under Grant No. B16F640076; Olle Engkvist Foundation under Grant No. 200-0605; STFC (United Kingdom); Suranaree University of Technology (SUT), Thailand Science Research and Innovation (TSRI), and National Science Research and Innovation Fund (NSRF) under Grant No. 160355; The Royal Society, UK, under Grants No. DH140054 and No. DH160214; The Swedish Research Council; U.S. Department of Energy under Grant No. DE-FG02-05ER41374.

APPENDIX: BRANCHING FRACTIONS OF THE KNOWN EXCLUSIVE $D^0(D^+)$ DECAYS INVOLVING $\pi^+\pi^+\pi^-$

Tables X and XI show the intermediate and final states that contribute to the inclusive decays $D^0 \to \pi^+\pi^+\pi^-X$ and $D^+ \to \pi^+\pi^+\pi^-X$ as well as the known branching fractions. The known branching fractions of $D^0 \to \pi^+\pi^+\pi^-X$ and $D^+ \to \pi^+\pi^+\pi^-X$ are $\mathcal{B}(D^0 \to \pi^+\pi^+\pi^-X) = (16.05 \pm 0.47)\%$ and $\mathcal{B}(D^+ \to \pi^+\pi^+\pi^-X) = (14.74 \pm 0.53)\%$, respectively.

TABLE X. The initial and final states contributing to the inclusive decay $D^0 \to \pi^+\pi^+\pi^-X$, along with the known branching fractions. The branching fractions of the hadronic D decays containing $\bar{K}^0$ have been obtained by scaling the known branching fractions of K^0_S by a factor of 2. Any π^+ or π^- from K^0_S decays have not been included. The contributions of some decays containing η, η', ω, and ϕ have been excluded to avoid overlaps among various decays.

Initial state	$\mathcal{B}^{\text{Initial}}(\%)$	Final state	$\mathcal{B}^{\text{Final}}(\%)$	References	Note
$K^-\pi^+\pi^+\pi^-$	8.220 ± 0.140	$K^-\pi^+\pi^+\pi^-$	8.168 ± 0.145	[5]	None ω
$K^-\pi^+\omega$	3.392 ± 0.096	$K^-\pi^+\pi^+\pi^-X$	3.088 ± 0.087	[6]	Scaled by $\mathcal{B}(\omega \to \pi^+\pi^-X) \sim 91.0\%$
$K^-\pi^+\pi^+\pi^-\pi^0$	4.300 ± 0.400	$K^-\pi^+\pi^+\pi^-\pi^0$	0.845 ± 0.409	[5]	None η, η', and ω
$\pi^+\pi^+\pi^-\pi^+$	0.755 ± 0.020	$\pi^+\pi^+\pi^-\pi^+$	0.755 ± 0.020	[5]	⋯
$K^-\pi^+\eta'$	0.643 ± 0.034	$K^-\pi^+\pi^+\pi^-X$	0.525 ± 0.028	[5]	Scaled by $\mathcal{B}(\eta' \to \pi^+\pi^-X) \sim 81.7\%$
$K^-\pi^+\eta$	1.880 ± 0.050	$K^-\pi^+\pi^+\pi^-X$	0.514 ± 0.013	[5]	Scaled by $\mathcal{B}(\eta \to \pi^+\pi^-X) \sim 27.4\%$
$K^{*-}\rho^0\pi^+$	0.320 ± 0.060	$K^{*-}\pi^+\pi^-\pi^+$	0.320 ± 0.060	[5]	Scaled by $\mathcal{B}(\rho^0 \to \pi^+\pi^-) \sim 100\%$
$\pi^+\pi^+\pi^-\pi^-\pi^0\pi^0$	0.442 ± 0.029	$\pi^+\pi^+\pi^-\pi^-\pi^0\pi^0$	0.317 ± 0.030	[7]	None η, η' and ω
$\pi^+\pi^+\pi^-\pi^-\pi^0$	0.420 ± 0.050	$\pi^+\pi^+\pi^-\pi^-\pi^0$	0.275 ± 0.053	[5]	None η, η', and ω
$K^0\eta'$	1.898 ± 0.045	$K^0\pi^+\pi^-\pi^+\pi^-X$	0.226 ± 0.005	[5]	Scaled by $\mathcal{B}(\eta' \to \pi^+\pi^-\eta) \times \mathcal{B}(\eta \to \pi^+\pi^-X) \sim 11.9\%$
$\bar{K}^0\rho^0\pi^+\pi^-$	0.220 ± 0.099	$\bar{K}^0\pi^+\pi^+\pi^-\pi^-$	0.220 ± 0.099	[5]	Scaled by $\mathcal{B}(\rho^0 \to \pi^+\pi^-) \sim 100\%$
$K^-\pi^+\pi^0\eta$	0.449 ± 0.027	$K^-\pi^+\pi^0\pi^+\pi^-X$	0.123 ± 0.007	[5]	Scaled by $\mathcal{B}(\eta \to \pi^+\pi^-X) \sim 27.4\%$
$\pi^+\pi^-\omega$	0.133 ± 0.020	$\pi^+\pi^-\pi^+\pi^-X$	0.121 ± 0.018	[5]	Scaled by $\mathcal{B}(\omega \to \pi^+\pi^-X) \sim 91.0\%$
$K^0\pi^+\pi^-\pi^+\pi^-$	<0.120	$K^0\pi^+\pi^-\pi^+\pi^-$	0.12	[5]	⋯
Others	0.543 ± 0.041	$\pi^+\pi^+\pi^-X$	0.434 ± 0.033	[5,7]	Dominated by $\pi^+\pi^-\eta X, \pi^+\pi^+\pi^-\eta' X, \eta\eta'$ and $\omega\eta \sim 80\%$
Sum	⋯	⋯	16.05 ± 0.47	⋯	⋯

TABLE XI. The initial and final states contributing to the inclusive decay $D^+ \to \pi^+\pi^+\pi^-X$, along with the known branching fractions. The branching fractions of the hadronic D decays containing $\bar{K}^0$ have been obtained by scaling the known branching fractions of K^0_S by a factor of 2. Any π^+ or π^- from K^0_S decays have not been included. The contributions of some decays containing η, η', ω, and ϕ have been excluded to avoid overlaps among various decays.

Initial state	$\mathcal{B}^{\rm Initial}(\%)$	Final state	$\mathcal{B}^{\rm Final}(\%)$	References	Note
$\bar{K}^0\pi^+\pi^+\pi^-$	6.200 ± 0.127	$\bar{K}^0\pi^+\pi^+\pi^-$	6.178 ± 0.130	[5]	None ω
$\bar{K}^0\pi^+\omega$	1.414 ± 0.071	$\bar{K}^0\pi^+\pi^+\pi^-X$	1.287 ± 0.053	[5]	Scaled by $\mathcal{B}(\omega \to \pi^+\pi^-X) \sim 91.0\%$
$\bar{K}^0\pi^+\pi^+\pi^-\pi^0$	3.056 ± 0.102	$\bar{K}^0\pi^+\pi^+\pi^-\pi^0$	1.198 ± 0.117	[8]	None η, η', and ω
$\pi^+\pi^+\pi^-\pi^0$	1.160 ± 0.080	$\pi^+\pi^+\pi^-\pi^0$	0.954 ± 0.083	[5]	None η, η', ω and ϕ
$\bar{K}^0\pi^+\eta$	2.620 ± 0.071	$\bar{K}^0\pi^+\pi^+\pi^-X$	0.718 ± 0.019	[5]	Scaled by $\mathcal{B}(\eta \to \pi^+\pi^-X) \sim 27.4\%$
$K^-\pi^+\pi^+\pi^+\pi^-$	0.570 ± 0.050	$K^-\pi^+\pi^+\pi^+\pi^-$	0.570 ± 0.050	[5]	...
$\pi^+\eta'$	0.497 ± 0.019	$\pi^+\pi^+\pi^-X$	0.406 ± 0.016	[5]	Scaled by $\mathcal{B}(\eta' \to \pi^+\pi^-X) \sim 81.7\%$
$\pi^+\pi^0\phi$	2.3 ± 1.0	$\pi^+\pi^0\pi^+\pi^-X$	0.362 ± 0.157	[5]	Scaled by $\mathcal{B}(\phi \to \pi^+\pi^-X) \sim 15.6\%$
$\pi^+\pi^0\omega$	0.39 ± 0.09	$\pi^+\pi^0\pi^+\pi^-X$	0.355 ± 0.082	[5]	Scaled by $\mathcal{B}(\omega \to \pi^+\pi^-X) \sim 91.0\%$
$\pi^+\pi^+\pi^-\pi^0\pi^0$	1.07 ± 0.41	$\pi^+\pi^+\pi^-\pi^0\pi^0$	0.322 ± 0.445	[5]	None η, η', ω and ϕ
$\bar{K}^0\pi^+\eta'$	0.380 ± 0.030	$\bar{K}^0\pi^+\pi^+\pi^-X$	0.311 ± 0.025	[5]	Scaled by $\mathcal{B}(\eta' \to \pi^+\pi^-X) \sim 81.7\%$
$\pi^+\pi^+\pi^-$	0.327 ± 0.018	$\pi^+\pi^+\pi^-$	0.305 ± 0.018	[5]	None ω
$\pi^+\pi^+\pi^-\pi^0\eta$	0.388 ± 0.032	$\pi^+\pi^+\pi^-\pi^0\eta$	0.251 ± 0.040	[7]	None η and η'
$\pi^+\pi^+\pi^-\pi^0\pi^0\pi^0$	0.347 ± 0.031	$\pi^+\pi^+\pi^-\pi^0\pi^0\pi^0$	0.250 ± 0.032	[7]	None η
$\pi^+\pi^+\pi^+\pi^-\pi^-$	0.166 ± 0.016	$\pi^+\pi^+\pi^+\pi^-\pi^-$	0.166 ± 0.016	[5]	...
$\pi^+\eta\eta$	0.296 ± 0.026	$\pi^+\eta\pi^+\pi^-X$	0.162 ± 0.014	[5]	Scaled by $\mathcal{B}(\eta \to \pi^+\pi^-X) \times 2 \sim 54.8\%$
$\pi^+\pi^+\pi^+\pi^-\pi^-\pi^0$	0.238 ± 0.022	$\pi^+\pi^+\pi^+\pi^-\pi^-\pi^0$	0.160 ± 0.023	[7]	None η
$\pi^+\pi^0\eta'$	0.16 ± 0.05	$\pi^+\pi^0\pi^+\pi^-X$	0.131 ± 0.041	[5]	Scaled by $\mathcal{B}(\eta' \to \pi^+\pi^-X) \sim 81.7\%$
$\pi^+\pi^+\pi^-\eta$	0.341 ± 0.021	$\pi^+\pi^+\pi^-\eta$	0.125 ± 0.023	[5]	None η'
$\pi^+\eta$	0.377 ± 0.009	$\pi^+\pi^+\pi^-X$	0.103 ± 0.003	[5]	Scaled by $\mathcal{B}(\eta \to \pi^+\pi^-X) \sim 27.4\%$
Others	0.532 ± 0.034	$\pi^+\pi^+\pi^-X$	0.426 ± 0.027	[5,7]	Dominated by $\pi^+\eta(\bar{K}^0\pi^0, \pi^0, \pi^0\pi^0, \pi^0\pi^0\pi^0)$ and $\pi^+\phi \sim 80\%$
Sum	...	...	14.74 ± 0.53	...	...

[1] Y. Amhis *et al.* (Heavy Flavor Averaging Group), Eur. Phys. J. C **81**, 226 (2021); updated results are available at https://hflav-eos.web.cern.ch/hflav-eos/semi/spring21/html/RDsDsstar/RDRDs.html.

[2] R. Aaij *et al.* (LHCb Collaboration), Phys. Rev. Lett. **120**, 171802 (2018).

[3] R. Aaij *et al.* (LHCb Collaboration), Phys. Rev. D **97**, 072013 (2018).

[4] M. Ablikim *et al.* (BESIII Collaboration), arXiv:2212.13072.

[5] P. A. Zyla *et al.* (Particle Data Group), Prog. Theor. Exp. Phys. **2022**, 083C01 (2022).

[6] M. Ablikim *et al.* (BESIII Collaboration), Phys. Rev. D **105**, 032009 (2022).

[7] M. Ablikim *et al.* (BESIII Collaboration), Phys. Rev. D **106**, 092005 (2022).

[8] M. Ablikim *et al.* (BESIII Collaboration), Phys. Rev. D **106**, 032002 (2022).

[9] M. Ablikim *et al.* (BESIII Collaboration), Chin. Phys. C **37**, 123001 (2013); Phys. Lett. B **753**, 629 (2016).

[10] M. Ablikim *et al.* (BESIII Collaboration), Nucl. Instrum. Methods Phys. Res., Sect. A **614**, 345 (2010).

[11] C. H. Yu *et al.*, in *Proceedings of IPAC2016, Busan, Korea* (JACoW, Geneva, Switzerland, 2016), https://accelconf.web.cern.ch/ipac2016/doi/JACoW-IPAC2016-TUYA01.html.

[12] K. X. Huang *et al.*, Nucl. Sci. Tech. **33**, 142 (2022).

[13] S. Agostinelli *et al.* (GEANT4 Collaboration), Nucl. Instrum. Methods Phys. Res., Sect. A **506**, 250 (2003).

[14] S. Jadach, B. F. L. Ward, and Z. Was, Comput. Phys. Commun. **130**, 260 (2000); Phys. Rev. D **63**, 113009 (2001).

[15] D. J. Lange, Nucl. Instrum. Methods Phys. Res., Sect. A **462**, 152 (2001); R. G. Ping, Chin. Phys. C **32**, 599 (2008).

[16] J. C. Chen, G. S. Huang, X. R. Qi, D. H. Zhang, and Y. S. Zhu, Phys. Rev. D **62**, 034003 (2000).

[17] R. L. Yang, R. G. Ping, and H. Chen, Chin. Phys. Lett. **31**, 061301 (2014).

[18] E. Richter-Was, Phys. Lett. B **303**, 163 (1993).

[19] R. M. Baltrusaitis *et al.* (Mark III Collaboration), Phys. Rev. Lett. **56**, 2140 (1986).

[20] J. Adler *et al.* (Mark III Collaboration), Phys. Rev. Lett. **60**, 89 (1988).

[21] T. Gershon, J. Libby, and G. Wilkinson, Phys. Lett. B **750**, 338 (2015).

[22] T. Evans, S. T. Harnew, J. Libby, S. Malde, J. Rademacker, and G. Wilkinson, Phys. Lett. B **757**, 520 (2016); **765**, 402(E) (2017).
[23] Heavy Flavor Averaging Group (HFLAV), http://www.slac.stanford.edu/xorg/hflav/charm/.
[24] M. Ablikim *et al.* (BESIII Collaboration), Phys. Rev. D **100**, 072006 (2019).
[25] M. Ablikim *et al.* (BESIII Collaboration), Phys. Rev. Lett. **121**, 171803 (2018).
[26] M. Ablikim *et al.* (BESIII Collaboration), Phys. Rev. Lett. **124**, 241803 (2020).
[27] H. Albrecht *et al.* (ARGUS Collaboration), Phys. Lett. B **241**, 278 (1990).
[28] M. Lefebvre, R. K. Keeler, R. Sobie, and J. White, Nucl. Instrum. Methods Phys. Res., Sect. A **451**, 520 (2000).
[29] M. Ablikim *et al.* (BESIII Collaboration), Phys. Rev. D **92**, 112008 (2015).